

Article

Determining the Composition of Carbonate Solvent Systems Used in Lithium-Ion Batteries without Salt Removal

Mohammad Parhizi¹, Louis Edwards Caceres-Martinez¹ , Brent A. Modereger², Hilikka I. Kenttämäa², Gozdem Kilaz^{1,*} and Jason K. Ostanek^{1,*} 

¹ School of Engineering Technology, Purdue University, 401 N. Grant St., West Lafayette, IN 47907, USA; mparhizi@purdue.edu (M.P.); lcaceres@purdue.edu (L.E.C.-M.)

² Department of Chemistry, Purdue University, 560 Oval Dr., West Lafayette, IN 47907, USA; bmodereger@purdue.edu (B.A.M.); hilikka@purdue.edu (H.I.K.)

* Correspondence: gkilaz@purdue.edu (G.K.); jostanek@purdue.edu (J.K.O.)

Abstract: In this work, two methods were investigated for determining the composition of carbonate solvent systems used in lithium-ion (Li-ion) battery electrolytes. One method was based on comprehensive two-dimensional gas chromatography with electron ionization time-of-flight mass spectrometry (GC×GC/EI TOF MS), which often enables unknown compound identification by their electron ionization (EI) mass spectra. The other method was based on comprehensive two-dimensional gas chromatography with flame ionization detection (GC×GC/FID). Both methods were used to determine the concentrations of six different commonly used carbonates in Li-ion battery electrolytes (i.e., ethylene carbonate (EC), propylene carbonate (PC), dimethyl carbonate (DMC), diethyl carbonate (DEC), ethyl methyl carbonate (EMC), and vinylene carbonate (VC) in model compound mixtures (MCMs), single-blind samples (SBS), and a commercially obtained electrolyte solution (COES). Both methods were found to be precise (uncertainty < 5%), accurate (error < 5%), and sensitive (limit of detection < 0.12 ppm for FID and < 2.7 ppm for MS). Furthermore, unlike the previously reported methods, these methods do not require removing lithium hexafluorophosphate salt (LiPF₆) from the sample prior to analysis. Removal of the lithium salt was avoided by diluting the electrolyte solutions prior to analysis (1000-fold dilution) and using minimal sample volumes (0.1 μL) for analysis.

Keywords: lithium-ion batteries; electrolyte; two-dimensional gas chromatography (GC×GC); mass spectrometry (MS); flame ionization detector (FID); analytical techniques



Citation: Parhizi, M.; Caceres-Martinez, L.E.; Modereger, B.A.; Kenttämäa, H.I.; Kilaz, G.; Ostanek, J.K. Determining the Composition of Carbonate Solvent Systems Used in Lithium-Ion Batteries without Salt Removal.

Energies **2022**, *15*, 2805.
<https://doi.org/10.3390/en15082805>

Academic Editors: Alon Kuperman and Alessandro Lampasi

Received: 7 March 2022

Accepted: 4 April 2022

Published: 12 April 2022

Publisher's Note: MDPI stays neutral with regard to jurisdictional claims in published maps and institutional affiliations.



Copyright: © 2022 by the authors. Licensee MDPI, Basel, Switzerland. This article is an open access article distributed under the terms and conditions of the Creative Commons Attribution (CC BY) license (<https://creativecommons.org/licenses/by/4.0/>).

1. Introduction

Lithium-ion (Li-ion) batteries are the predominant energy storage and conversion device in various applications, such as portable consumer electronics, electric vehicles (EVs), grid storage, space applications, and military applications [1–3]. Li-ion batteries offer several advantages over other rechargeable batteries, such as high energy density and power density, low self-discharge rate, and long life [4]. However, decomposition reactions occur within Li-ion batteries under certain operating conditions, which negatively impact the performance of the battery and impose safety hazards by generating toxic and flammable compounds. For instance, under abuse conditions, decomposition reactions generate a significant amount of heat and gaseous products, leading the cell into thermal runaway. Thermal runaway is frequently accompanied by the release of flammable and toxic gases during the venting process and afterward. The rates and pathways of these decomposition reactions, the composition and amount of the gaseous products, and heat generation rates are affected by the solvent(s) used within the electrolyte solution, which can vary significantly [5]. The most common electrolytes used in Li-ion batteries comprise a conducting salt such as lithium hexafluorophosphate (LiPF₆) dissolved in a mixture of organic carbonate solvents.

Accurate analytical methods for determining the composition of solvent systems used in Li-ion batteries are needed to better understand decomposition processes occurring within Li-ion batteries and their effects on battery performance and safety. Recovering organic carbonate compounds during recycling may also benefit from accurate analytical methods to verify the solvent composition [6]. Several studies have implemented different analytical methods to identify and quantify electrolyte components. For example, in a qualitative study, Horsthemke et al. [7] used gas chromatography combined with mass spectrometry (GC/MS) to identify electrolyte components and aging products for various commercially available Li-ion cells. A headspace solid-phase microextraction (SPME) technique was used to prevent the injection of salts into the GC column [7]. On the other hand, Ellis et al. [8] have used Fourier-transform infrared (FTIR) spectroscopy to determine the concentrations of LiPF_6 and common solvents in Li-ion battery electrolytes. An FTIR spectral database of known solutions with known concentrations was first created. Machine learning was then used to quantify unknown electrolyte solutions by interpolating data in the FTIR spectral database [8]. Further, Gachot et al. [9] have used the GC/MS technique to identify the compounds within the Li-ion battery electrolytes after cycling and heating. A postcapillary column was used to preserve the ion source from HF and the bleeding of the first column. The same research group has coupled gas chromatography with mass spectrometry and Fourier transform infrared spectroscopy (GC/MS-FTIR) to identify electrolyte compositions. This method was used to characterize volatile compounds released during thermal runaway and gaseous and soluble volatile products in a swollen battery [10]. Schultz et al. [11] have employed high-performance liquid chromatography (HPLC) coupled to tandem mass spectrometry (LC/MS/MS) for the identification and quantification of components of Li-ion battery electrolytes. The method was then used to quantify chemical species produced under different aging processes [11]. Petibon et al. [12] have developed a semi-quantitative approach based on the GC/MS technique for the determination of the consumption and transesterification of additives and solvents after formation cycles and storage at high potential. Liquid–liquid extraction was used to remove LiPF_6 prior to analysis [12]. However, liquid–liquid extraction is time-consuming and may introduce additional uncertainty in the measurement. Terborg et al. [13] have employed GC/MS and GC/FID to identify organic solvents in Li-ion battery electrolytes. Thompson et al. [14] have used GC/MS to analyze the changes in the composition of the carbonates within the battery electrolytes after cycling at different cutoff potentials. The salt was extracted from the samples using liquid–liquid extraction and centrifuge [14]. Weber et al. [15] have used a GC–MS-based analytical method to identify phosphorous/organic degradation products in aged cells that are known to be toxic. Quantification of dimethyl phosphorofluoridate (DMPF) and diethyl phosphorofluoridate (DEPF) has been done using calibration curves [15]. Finally, several previous studies have used gas chromatography to investigate venting behavior and venting gas composition of lithium-ion cells during thermal runaway [10,16–19].

Most of the previously reported techniques required removing LiPF_6 salt from the samples prior to analysis because it is well known that the conductive salt reacts with the silicon coating of the GC column and results in excessive column bleeding [7]. However, salt removal is time-consuming, introduces additional costs, and reduces the precision of the method.

Comprehensive two-dimensional gas chromatography ($\text{GC} \times \text{GC}$) coupled with FID ($\text{GC} \times \text{GC}/\text{FID}$), or mass spectrometry detection ($\text{GC} \times \text{GC}/\text{EI TOF MS}$) is a powerful analytical technique due to its high resolution and high peak capacity. MS can often be used for the identification of unknown compounds based on a comparison of their electron ionization (EI) mass spectra to mass spectral libraries, while FID is often used for compound quantification because of the similar response of FID to different types of compounds. In this paper, two methods are described for the determination of the compositions of solvent systems used in Li-ion battery electrolytes, one based on $\text{GC} \times \text{GC}/\text{FID}$ and the other $\text{GC} \times \text{GC}/\text{EI TOF MS}$. $\text{GC} \times \text{GC}$ has been widely used to analyze complex mixtures related

to food, petrochemical, environmental, biomedical, hardware, and software industries [20]. However, to the best of the authors' knowledge, determination of the compositions of the solvent systems used in Li-ion battery electrolytes has not been performed based on GC×GC/FID or GC×GC/EI TOF MS. The purpose of the present work was to determine the accuracy and precision of these two analytical techniques when analyzing compounds found in electrolyte solutions of Li-ion batteries. To quantify and compare the performance of the two analytical techniques, the limit of detection (LOD), limit of quantification (LOQ), uncertainty, and repeatability were determined.

2. Experimental

2.1. Chemicals

Ethylene carbonate (EC; ≥99%), propylene carbonate (PC; ≥99%), dimethyl carbonate (DMC; 99.9%), diethyl carbonate (DEC; ≥99%), ethyl methyl carbonate (EMC; 99.9%), vinylene carbonate (VC; 99.5%), a commercially available Li-ion battery electrolyte comprised of a 1.0 M (±0.1 M) LiPF₆ solution in 50/50 (v/v) (±5%) EC and DMC, a commercially available Li-ion battery electrolyte comprised of a 1.0 M (±0.1 M) LiPF₆ solution in 50/50 (v/v) (±5%) EC and DEC, and a commercially available Li-ion battery electrolyte comprised of a 1.0 M (±0.1 M) LiPF₆ solution in 50/50 (v/v) (±5%) EC and EMC were purchased from Sigma-Aldrich (St. Louis, MO, USA). Dichloromethane (DCM) (ACROS Organics; ≥99.9%) and acetone (Honeywell Burdick & Jackson; ≥99.9%) were purchased from Fisher Scientific (Branchburg, NJ, USA). Isopropanol (IPA; 99.8%) was purchased from Techspray (Kennesaw, GA, USA). All chemicals were used as received.

2.2. Carbonate Mixtures and Li-Ion Battery Electrolyte

Various model mixtures of known carbonates were used to determine the accuracy and precision of the GC×GC/FID and GC×GC/EI TOF MS methods. Model compound mixtures (MCMs) with three different compositions were prepared and analyzed (MCM #1, MCM #2, and MCM #3; Table 1). One MCM was prepared and analyzed on three different days (MCM #1A MCM #2A, and MCM #3A; Table 1) to determine the intraday repeatability of the methods. A commercially obtained electrolyte solution (COES) of 1.0 M LiPF₆ solution in 50:50 (v/v) (±5%) EC and DMC was purchased from Sigma-Aldrich and analyzed using both methods (Table 1). Two single-blind samples (SBSs) were also analyzed (using both methods) that were prepared by members of a different laboratory with compositions that were revealed only after they were analyzed (SBS; Table 1). SBS #1 was prepared with pure EC (≥99%), EMC (≥99.9%), VC (≥99.5%), and isopropanol (IPA; 99.8%). SBS #2 was prepared from an electrolyte solution in 50:50 (v/v) (±5%) EC and EMC, an electrolyte solution in 50:50 (v/v) (±5%) EC and DEC, and pure VC (≥99.5%). SBS #1 and SBS#2 were shipped (~3 h) then stored (up to 6 months) prior to preparation and injection. Samples were prepared by diluting 10 µL of each mixture in 10 mL DCM or acetone. Each sample was injected 10 times into both instruments with an injection volume of 0.1 µL and a split ratio of 24.

Table 1. Composition of various mixtures analyzed by GC×GC/FID and GC×GC/EI TOF MS methods.

Mixture	Volume Percentages %							LiPF ₆	IPA
	EC	EMC	DMC	DEC	PC	VC			
MCM #1A	-	20.0	20.0	20.0	20.0	20.0	-	-	
MCM #1B	-	20.0	20.0	20.0	20.0	20.0	-	-	
MCM #1C	-	20.0	20.0	20.0	20.0	20.0	-	-	
MCM #2	-	20.0	60.0	-	-	20.0	-	-	
MCM #3	60.0	20.0	-	-	20.0	-	-	-	
SBS #1	27.8	55	-	-	-	2.8	-	14.4	
SBS #2	42.8	21.4	-	21.4	-	4.7	9.6	-	
COES	45.0	-	45.0	-	-	-	10.0	-	

2.3. GC×GC/FID Instrument Operating Conditions and Parameters

All GC×GC/FID measurements were performed using an instrument composed of a 7890B GC oven (Agilent, Santa Clara, CA, USA), a 7683 series autosampler (Hewlett-Packard, Palo Alto, CA, USA), a 7683B series injector (Agilent, Santa Clara, CA, USA), an FID (Agilent, Santa Clara, CA, USA), and a quad-jet dual-stage thermal modulator (LECO Corporation, Saint Joseph, MI, USA) cooled with liquid nitrogen. The capillary column contained within the primary oven (primary column) was a midpolar 30 m DB-17MS column. The capillary column contained within the secondary oven (secondary column) was a nonpolar 0.8 m DB-1MS column. A 0.3 m guard column (Ultimate Plus Deactivated Fused Silica) was used between the secondary column and the FID. All columns had a 0.25 mm inner diameter and a 0.25 µm film thickness (Agilent, Santa Clara, CA, USA). Ultra-high purity (99.9999%) helium was used as the carrier gas, with a flow rate of 1.5 mL/min. Primary oven temperature was maintained at 40 °C for 1.0 min, increased to 200 °C at a temperature ramp rate of 3 °C/minute, and then held constant for five more minutes. The temperature offsets (relative to the primary oven) for the secondary oven and modulator were +5 °C and +15 °C, respectively. The modulation period was 3.0 s, with a hot pulse duration of 0.9 s. The temperatures of the FID and the inlet of the injection port were 300 °C and 280 °C, respectively. The acquisition rate of the FID was 200 Hz, and the acquisition solvent delay was 150 s. The injection volume was 0.1 µL. The split-ratio for the inlet of the injection port was 24. The instrument was operated using ChromaTOF software (version 4.71.0.0). A S/N threshold of 50 was used for data processing of all chromatograms.

2.4. GC×GC/EI TOF MS Instrument Operating Conditions and Parameters

All GC×GC/EI TOF MS measurements were performed using a Pegasus GC-HRT 4D (LECO, Saint Joseph, MI, USA), which was composed of a 7890B GC oven (Agilent, Santa Clara, CA, USA), an Agilent injector (G4513A), a quad-jet dual-stage thermal modulator (LECO, Saint Joseph, MI, USA) cooled with liquid nitrogen, an electron ionization source (LECO, Saint Joseph, MI, USA), and a high-resolution time-of-flight mass spectrometer (LECO, Saint Joseph, MI, USA). The capillary column contained within the primary oven (primary column) was a polar 60.0 m ZB-35HT column. The capillary column contained within the secondary oven (secondary column) was a nonpolar 1.2 m ZB-1HT column. All columns had a 0.25 mm inner diameter and a 0.25 µm film thickness (Phenomenex, Torrance, CA, USA). Ultra-high purity (99.9999%) helium was used as a carrier gas with a flow rate of 1.25 mL/minute. Primary oven temperature was maintained at 40 °C for 1.0 min, increased to 200 °C at a temperature ramp rate of 3 °C/min, and then held constant for five more minutes. The temperature offsets (relative to the primary oven) for the secondary oven and modulator were +5 °C and +15 °C, respectively. The modulation period was 3.0 s, with a hot pulse duration of 0.9 s. The temperatures of the transfer line and the inlet of the injection port were 300 °C and 280 °C, respectively. The temperature of the ion source was maintained at 200 °C. The kinetic energy of the electrons used for electron ionization (EI) was 70 eV. The acquisition solvent delay was 150 s. The injection volume was 0.1 µL. The split-ratio for the inlet of the injection port was 24. The instrument was operated using ChromaTOF software (version 1.90.60.0.43266). A S/N threshold of 50 was used for data processing of all chromatograms. The ChromaTOF software automatically identified compounds by comparing their EI mass spectra to the EI mass spectra in the Wiley (2011) and NIST (2011) databases. The match factor threshold, which is the minimum match factor an EI mass spectrum must exhibit with a database entry for a compound to be identified, was 800.

2.5. Calibration Curves and Sample Preparation

Calibration curves were established for each carbonate (DMC, DEC, PC, EMC, VC, and EC) by preparing a stock solution that had the same concentration of each carbonate as the pure carbonate solution prepared for analysis (discussed in Sections 2.3 and 2.4), which corresponded to 100% (v/v), and diluting the stock solution in DCM or acetone to prepare

solutions corresponding to 1, 5, 10, 20, 40, 60, and 80% (*v/v*) used for calibration. The stock solution was prepared by dissolving 200 μL of DMC, DEC, PC, EMC, VC, and 264.2 mg of EC (equivalent to 200 μL considering $\rho_{\text{EC}} = 1.321 \text{ g/cm}^3$) in 200 mL of acetone. Each calibration curve solution was then analyzed with GC \times GC/FID and GC \times GC/EI TOF MS according to Sections 2.3 and 2.4, respectively. The concentration of each carbonate in each calibration curve solution is shown in Table 2. In addition, each of the calibration curve solutions was analyzed five times with GC \times GC/FID and five times with GC \times GC/EI TOF MS. SBSs, MCMs, and COES were analyzed 10 times each with GC \times GC/FID and ten times each with GC \times GC/EI TOF MS.

Table 2. Concentrations of carbonates in calibration solutions.

Calibration Solution	Concentration [ppm]					
	DMC	EMC	DEC	VC	PC	EC
100%	1045.0	1005.0	965.0	1370.0	1221.0	1321.0
80%	836.0	804.0	772.0	1096.0	976.8	1056.8
60%	627.0	603.0	579.0	822.0	732.6	792.6
40%	418.0	402.0	386.0	548.0	488.4	528.4
20%	209.0	201.0	193.0	274.0	244.2	264.2
10%	104.5	100.5	96.5	137.0	122.1	132.1
5%	52.3	50.3	48.3	68.5	61.1	66.1
1%	10.5	10.1	9.7	13.7	12.2	13.2

2.6. Identification and Quantitation of the Carbonates

Testing the ability of GC \times GC/FID to identify the carbonates was carried out by preparing samples of individual carbonates, i.e., 10 μL of DMC, DEC, PC, EMC, VC, and 13.21 mg of EC in 10 mL acetone, and injecting them separately into the GC \times GC system to create a map for individual carbonates based on their first and second-retention times. Testing the GC \times GC/EI TOF MS method was based on the comparison of the measured EI mass spectra to the EI mass spectral library. Testing the quantitation of DMC, DEC, PC, EMC, VC, and EC was carried out by exporting the peak areas for each carbonate in the calibration solutions after data processing in GC \times GC/FID and GC \times GC/EI TOF MS to Microsoft Excel 365. The slope and intercept associated with the calibration curve of each compound were then determined using conventional linear regression analysis.

2.7. LOD and LOQ

The statistical LOD and LOQ for each compound was determined based on the standard deviation (σ) of the intercept over the slope (M) in the calibration curve data by using Equations (1) and (2), respectively [21].

$$\text{LOD} = 3.3 * \left(\frac{\sigma_{\text{intercept}}}{M} \right) \quad (1)$$

$$\text{LOQ} = 10.0 * \left(\frac{\sigma_{\text{intercept}}}{M} \right) \quad (2)$$

In order to accurately determine LOD and LOQ, additional solutions with lower concentrations, i.e., 0.1%, 0.2%, 0.4%, 0.6%, and 0.8% (*v/v*), were analyzed and data added to the original 8-point calibration curves.

2.8. Analysis of Column Bleeding

Aiming to determine whether the samples containing LiPF_6 salt cause excessive column bleeding, an experiment was carried out by injecting a blank acetone sample (considered as the baseline sample) before and after five injections of COES and SBS #2. All chromatograms were inspected for any visual signs of column bleed, changes in peak shapes, or changes in retention times.

2.9. Uncertainty Analysis

The uncertainty analysis was carried out similar to a method proposed by Moffat [22]. In the present work, an uncertainty analysis was performed in two steps. First, the uncertainty of the calibration curves was quantified. Second, the uncertainty of sample concentrations was quantified. Figure 1 presents the calibration curve for VC with a slope of m and an intercept of b . The slope and the intercept depend on the concentrations of the compound and the measured GC peak areas. However, both the concentrations and measured peak areas are subject to experimental uncertainties. In other words, the concentrations (x -axis) are subject to fixed errors (B) due to the sample preparation process, and the measured peak areas (y -axis) are subject to random errors (S) due to the repeated measurements. Thus, there is an overall uncertainty associated with the slope and the intercept of each calibration curve.

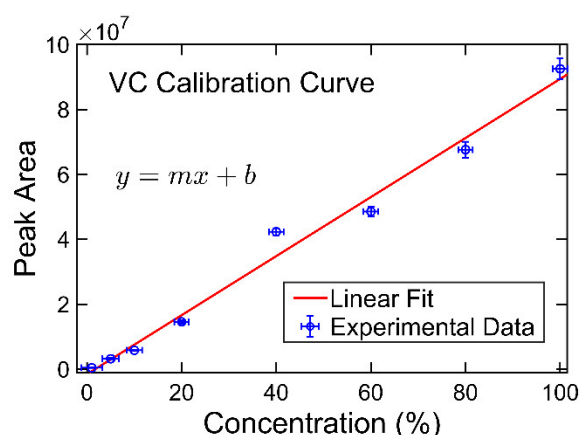


Figure 1. Calibration curve of vinylene carbonate (VC) with 95% confidence intervals.

The fixed and random uncertainties of the slope (B_{Rm} and S_{Rm} , respectively) and the intercept (B_{Rb} and S_{Rb} , respectively) of each calibration curve were determined with Equations (3) and (4), similar to Moffat et al. [22]:

$$B_{Rm} = \left\{ \sum_{i=1}^8 \left(\frac{\partial m}{\partial x_i} B_i \right)^2 \right\}^{\frac{1}{2}} \quad S_{Rm} = \left\{ \sum_{i=1}^8 \left(\frac{\partial m}{\partial y_i} S_i \right)^2 \right\}^{\frac{1}{2}} \quad (3)$$

$$B_{Rb} = \left\{ \sum_{i=1}^8 \left(\frac{\partial b}{\partial x_i} B_i \right)^2 \right\}^{\frac{1}{2}} \quad S_{Rb} = \left\{ \sum_{i=1}^8 \left(\frac{\partial b}{\partial y_i} S_i \right)^2 \right\}^{\frac{1}{2}} \quad (4)$$

where $B_i = \left\{ \sum (B_n)^2 \right\}^{\frac{1}{2}}$ was the overall fixed error arising from preparation of the solution with concentration of i . The subscript n referred to the number of pieces of equipment used in the process of preparing the i solution. $S_i = \frac{S_i}{\sqrt{N}}$ was the mean precision index calculated as the ratio of S_i , which was the standard deviation of the i solution, and N , which was the number of measurements made.

The overall uncertainty of the slope (U_{Rm}) and intercept (U_{Rb}) were calculated with Equation (5):

$$U_{Rm} = \sqrt{B_{Rm}^2 + (t \cdot S_{Rm})^2} \quad U_{Rb} = \sqrt{B_{Rb}^2 + (t \cdot S_{Rb})^2} \quad (5)$$

where t was the student's multiplier for 95% confidence, which for $N = 3, 5,$ and 10 , was $4.303, 2.776, 2.365, 2.262$ [23].

From the calibration curves, the concentration of each compound can be determined as $x = (y - b)/m$. Note that y is the measured peak area with a precision index (random

error), b is the intercept with fixed errors, and m is the slope with fixed errors. Therefore, the fixed and random error associated with concentration, x , can be determined as follows:

$$B_R = \sqrt{\left(\frac{\partial x}{\partial m} U_{Rm}\right)^2 + \left(\frac{\partial x}{\partial b} U_{Rb}\right)^2} \quad S_R = \sqrt{\left(\frac{\partial x}{\partial y} S_y\right)^2} \quad (6)$$

The total uncertainty associated with concentration of a compound, x , can be written as:

$$U_x = \sqrt{B_R^2 + (t \times S_R)^2} \quad (7)$$

3. Results and Discussion

3.1. Testing the Accuracy of Identification and Quantitation of Carbonates by Using GC×GC/FID

Carbonate compounds were identified using GC×GC/FID, based on their first- and second-dimension retention times (1D-RT and 2D-RT) of each carbonate. Figure 2 shows a three-dimensional chromatogram obtained by using GC×GC/FID for the 100% calibration solution. All the compounds were completely separated by GC×GC, allowing each carbonate to be detected without interference from the others. Table 3 summarizes the retention times as well as the slope and the Y-intercept for the calibration curve of each carbonate. Linear correlation coefficients (R^2) were found to be greater than 0.977 for all cases.

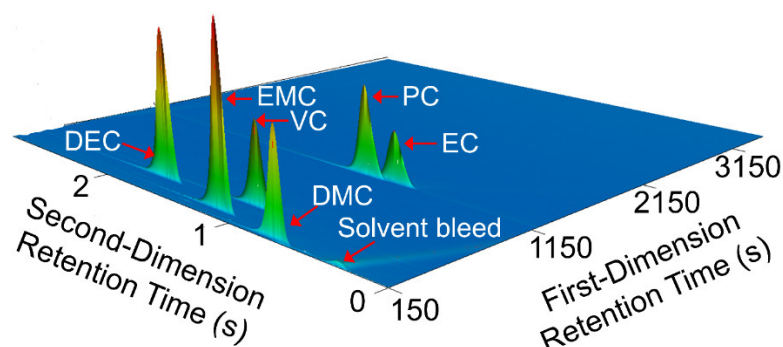


Figure 2. Three-dimensional chromatogram exhibiting effective separation of the carbonates in the 100% calibration solution when using the GC×GC/FID system.

Table 3. GC×GC/FID calibration results including the retention times and linear correlation parameters for common organic solvents found in Li-ion batteries.

Compound	1D-RT (s)	2D-RT (s)	Slope	Y-Intercept	R^2
DMC	171	0.695	9.82×10^7	-7.79×10^5	0.9987
EMC	240	1.160	1.89×10^8	-7.07×10^5	0.9970
DEC	351	1.740	2.00×10^8	-4.17×10^6	0.9952
VC	408	1.085	9.09×10^7	-1.53×10^6	0.9867
PC	1194	1.090	1.38×10^8	2.27×10^6	0.9774
EC	1206	0.890	8.36×10^7	-2.98×10^5	0.9831

3.2. LOD and LOQ of the GC×GC/FID Method

As shown in Figure 3, the minimum concentration of all the carbonate solvents, i.e., DMC, EMC, DEC, VC, PC, and EC, visually detected by the GC×GC/FID method was 0.2% at a signal to noise ratio of 50, corresponding to injections of 0.084, 0.080, 0.077, 0.110, 0.098, and 0.106 ppm in acetone for DMC, EMC, DEC, VC, PC, and EC, respectively.

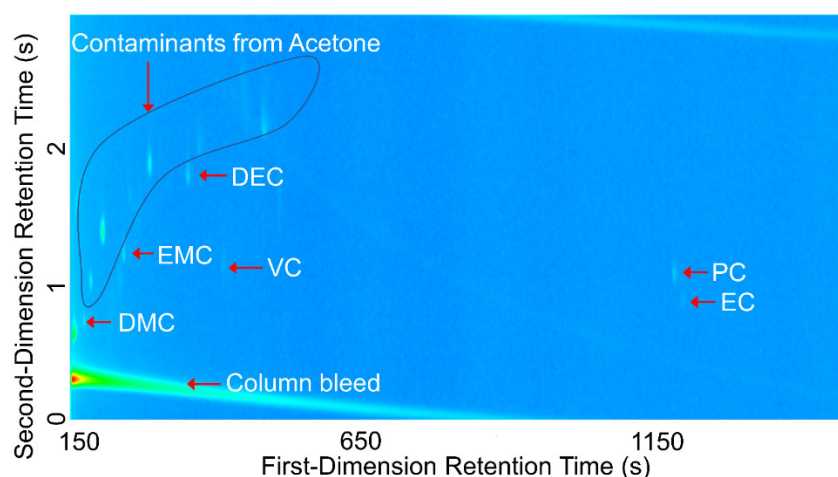


Figure 3. GC×GC/FID chromatogram of 0.2% (*v/v*) solution of DMC, EMC, DEC, VC, PC, and EC in acetone.

The statistical LOD and LOQ were determined using Equations (1) and (2), respectively. The visual LOD, statistical LOD, and statistical LOQ are summarized in Table 4. EC and EMC have the highest and lowest LOD and LOQ, respectively. These LODs are much lower than the LODs reported for one-dimensional gas chromatography with FID [13]. The LOQ for EMC, DEC, DMC, VC, PC, and EC were 3.04, 3.60, 4.23, 11.43, 12.13, and 16.41 ppm, respectively.

Table 4. Limit of detection (LOD) and limit of quantification (LOQ) of DMC, EMC, DEC, VC, PC, and EC when using GC×GC/FID.

Compound	Visual LOD (ppm)	Statistical LOD (ppm)	LOQ (ppm)
DMC	0.08	1.40	4.23
EMC	0.08	1.00	3.04
DEC	0.08	1.19	3.60
VC	0.11	3.77	11.43
PC	0.10	4.00	12.13
EC	0.11	5.41	16.41

3.3. Testing the Accuracy of the Identification and Quantitation of Carbonates by Using GC×GC/EI TOF MS

Figure 4 shows the electron ionization (EI) mass spectra obtained by using GC×GC/EI TOF MS for DMC, EMC, DEC, VC, PC, and EC in the 100% calibration solution. The similarity factors upon comparison of the measured mass spectra to mass spectral libraries for DMC, EMC, DEC, VC, PC, and EC were 864, 808, 941, 888, 895, and 929, respectively. Table 5 summarizes the retention times as well, as the slopes and the y-intercepts of the calibration plots for each carbonate. Correlation coefficients for the linear regression of GC×GC/EI TOF MS peak area to compound concentration ranged from 0.9533 for DMC to 0.9990 for PC.

Table 5. GC×GC/EI TOF MS calibration results, including the retention times and linear correlation parameters for common organic solvents found in Li-ion batteries.

Compound	1D-RT (s)	2D-RT (s)	Slope	Y-Intercept	R ²
DMC	357	1.64	1.82×10^6	5.75×10^4	0.9533
EMC	467	1.85	2.23×10^6	-1.27×10^4	0.9547
DEC	636	2.05	2.43×10^6	-6.25×10^3	0.9606
VC	665	1.79	3.15×10^6	6.05×10^4	0.9943
PC	1526	1.77	1.50×10^6	3.22×10^3	0.9990
EC	1502	1.71	1.72×10^6	-6.01×10^4	0.9981

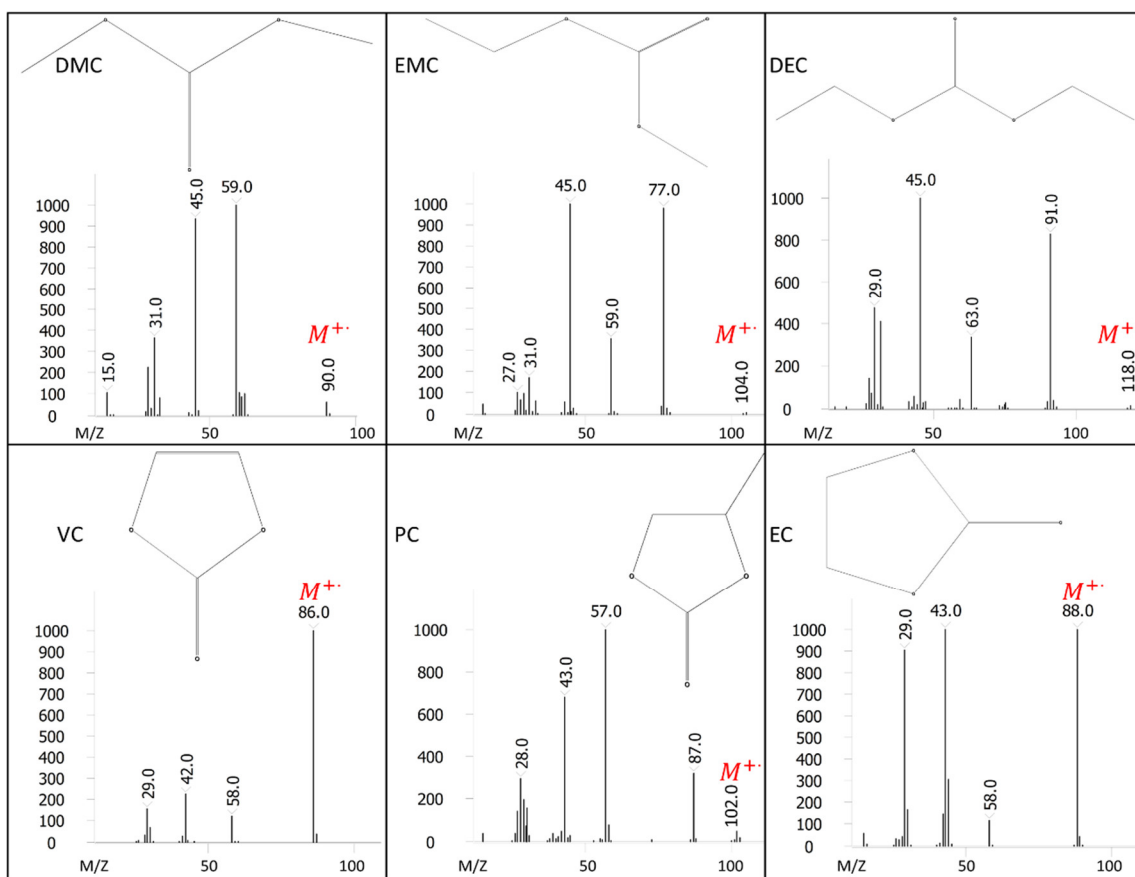


Figure 4. 70 eV EI mass spectra obtained by using GC×GC/EI TOF MS for DMC, EMC, DEC, VC, PC, and EC.

3.4. LOD and LOQ of the GC×GC/EI TOF MS Method

Carbonates in the solutions with the lowest concentrations, i.e., 0.1%, 0.2%, 0.4%, 0.6%, and 0.8% (*v/v*) were not detected by GC×GC/EI TOF MS. The minimum concentration (*v/v*) detected was for the 1% calibration solution (corresponding to injection of 0.42, 0.40, 0.39, and 0.55 ppm of DMC, EMC, DEC, and VC, respectively) or 5% (*v/v*) (corresponding to injection of 2.44 and 2.66 ppm of PC, and EC, respectively). The LOD and LOQ for the GC×GC/EI TOF MS method are summarized in Table 6. The statistical LOD was the greatest for DMC, EMC, DEC, and VC and lower for PC and EC. Statistical LOD was lower than the visual LOD for PC and EC. No solutions were prepared at concentrations between 1–5% for PC and EC. The LODs and LOQs were generally lower for the GC×GC/FID method than they were for the GC×GC/EI TOF MS method.

Table 6. Limit of detection (LOD) and limit of quantification (LOQ) for DMC, EMC, DEC, VC, PC, and EC obtained using the GC×GC/EI TOF MS method.

Compound	Visual LOD (ppm)	Statistical LOD (ppm)	LOQ (ppm)
DMC	0.42	6.58	19.95
EMC	0.40	6.92	20.97
DEC	0.39	5.56	16.84
VC	0.55	3.23	9.80
PC	2.44	1.55	4.70
EC	2.66	2.05	6.21

3.5. Testing the Accuracy of the Quantitation of MCMs

The intraday repeatability of quantitation was determined for both methods by measuring three samples that were prepared in the same way but on different days. The compositions determined for MCM #1A, MCM #1B, and MCM #1C are shown in Table 7. The results for MCM #1A–C were similar. The average volume percentage determined using GC×GC/FID for DMC, DEC, EMC, VC, and PC were 19.6 ± 2.4 , 20.5 ± 1.5 , 19.3 ± 0.8 , 19.3 ± 3.1 , and $20.9 \pm 1.9\%$ (*v/v*), respectively. The average volume percentage determined using GC×GC/EI TOF MS for DMC, DEC, EMC, VC, and PC were 17.0 ± 1.5 , 20.2 ± 1.3 , 21.6 ± 1.6 , 20.1 ± 1.4 , and $19.8 \pm 1.9\%$ (*v/v*), respectively. Measurements made on the same day were similar to each other (average relative standard deviation = 3.9%). In general, both instruments predicted the volume percentages of the carbonates with good accuracy. The largest error for the GC×GC/FID method was observed for PC, and the largest error observed for the GC×GC/EI TOF MS method was associated with DMC.

Table 7. Volume fraction of the components in MCM #1A–C measured using GC×GC/FID and GC×GC/EI TOF/MS. The expected concentration of each carbonate was $20 \pm 1.5\%$ for MCM#1A–C.

MCM	Injection	Volume Percentages MCM #1									
		DMC %		DEC %		EMC %		VC %		PC %	
		MS	FID	MS	FID	MS	FID	MS	FID	MS	FID
#1A	1	17.2	19.5	19.9	20.1	21.0	17.1	20.0	19.1	20.2	17.4
	2	17.2	20.2	20.5	20.6	21.5	17.6	20.5	19.8	20.8	17.7
	3	17.2	19.2	20.4	20.5	20.9	20.6	20.0	18.0	20.1	17.7
#1B	1	16.9	19.2	19.9	20.6	22.1	19.9	19.8	21.0	19.5	23.3
	2	17.3	19.4	19.9	20.6	21.9	20.4	19.7	21.4	19.5	23.3
	3	17.0	19.2	19.5	20.8	21.6	19.7	19.3	18.6	19.4	23.8
#1C	1	17.1	20.0	20.4	20.7	22.4	19.1	20.2	18.4	20.2	22.2
	2	16.6	19.9	20.6	20.6	21.5	19.1	20.8	18.6	19.5	21.6
	3	16.9	19.9	20.3	20.3	21.4	20.1	21.0	18.5	19.3	21.2

Additional MCMs were also analyzed using GC×GC/FID. The compositions determined for MCM #2 and MCM #3 are shown in Figure 5. MCM #2 was 20, 20, and 60% EMC, VC, and DMC, respectively. MCM #3 was 60, 20, and 20% EC, DEC, and PC, respectively. The uncertainties associated with the measurement of each compound and the actual concentration are also shown in Figure 5. The percentage errors of the GC×GC/FID method for EMC, VC, and EC in MCM #2, were 1.1, 0.7, 0.4%, respectively (average percentage error = 0.7%). The percentage errors of the GC×GC/FID method for EC, DEC, and PC in MCM #3, were 2.6, 3.1, 2.8%, respectively (average percentage error = 2.8%). Furthermore, the greatest uncertainty associated with the measurements was 4.1% for DMC in MCM #2, and 4.3% for EC in MCM #3.

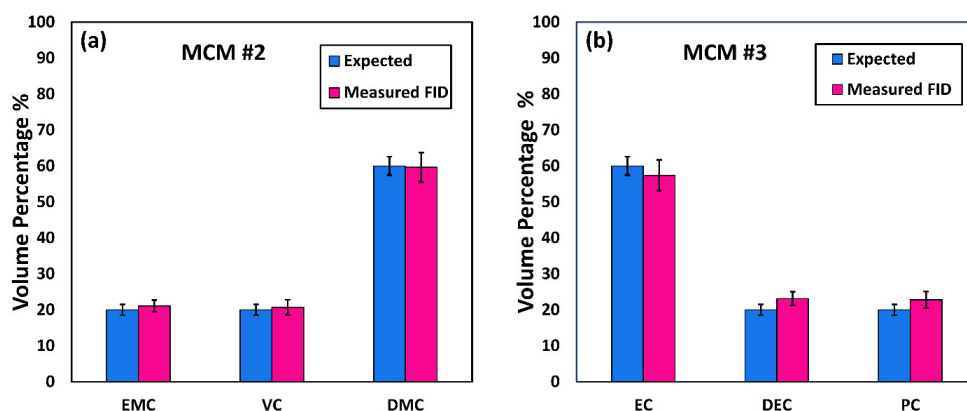


Figure 5. Expected and measured volume percentages of carbonates in MCM #2 (a) and MCM #3 (b) determined with GC×GC/FID.

3.6. Testing the Accuracy of Quantitation of SBSs and COES

The compositions determined for SBSs and COES are shown in Figure 6. The errors in the expected volume percentages of the electrolytes in SBS #2 (which was prepared with a commercially obtained electrolyte solution as described in the experimental section) and the COES were especially large because of large uncertainties mentioned in the product specifications from the manufacturer. Both methods were very accurate. The percentage errors of the GC×GC/FID method for EC, EMC, and VC in SPS #1 were 0.8, 1.0, and 0.4%, respectively (average percentage error = 0.8%). The percentage errors of the GC×GC/FID method for EC, DEC, EMC, and VC in SPS #2 were 1.2, 2.0, 6.4, and 0.3%, respectively (average percentage error = 2.5%). The percentage errors of the GC×GC/FID method for EC and DMC in COES were 2.5 and 5.7%, respectively (average percentage error = 4.1%). The percentage errors of the GC×GC/EI TOF MS method for EC, EMC, and VC in SPS #1 were 0.2, 2.4, and 1.9%, respectively (average percentage error = 1.5%). The percentage errors of the GC×GC/EI TOF MS method for EC, DEC, EMC, and VC in SPS #2 were 1.8, 2.9, 2.6, and 0.2%, respectively (average percentage error = 1.9%). The percentage errors of the GC×GC/EI TOF MS method for EC and DMC in COES were 11 and 2%, respectively (average percentage error = 6.5%). Furthermore, the maximum uncertainty associated with the measurements using GC×GC/FID was 5.5% for DMC in COES (average uncertainty = 2.43%), and the maximum uncertainty of the measurements using GC×GC/EI TOF MS was 4.4% for EMC in SBS #1 (average uncertainty = 2.13%).

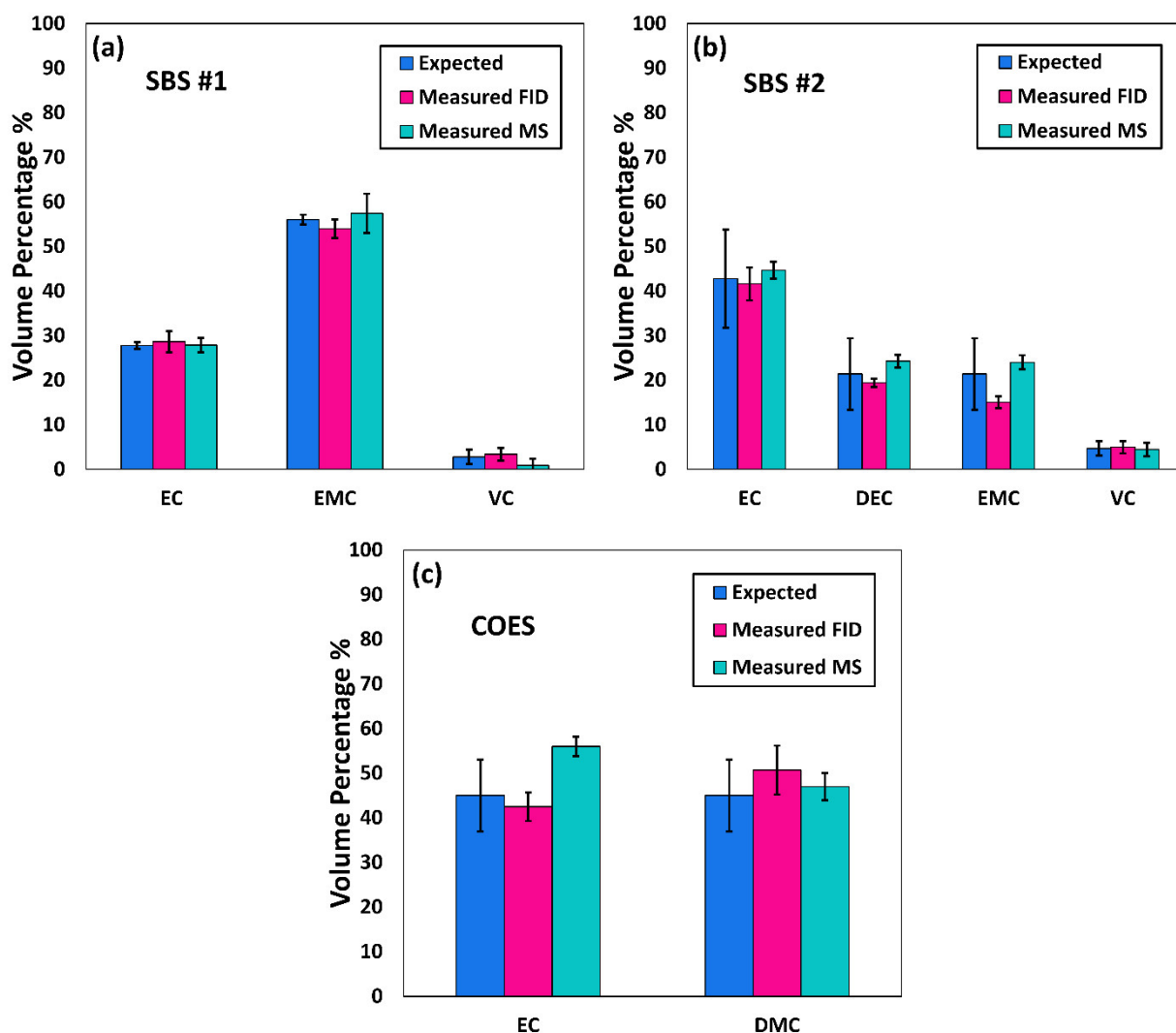


Figure 6. Volume percentages determined for carbonates in SBS #1 (a), SBS #2 (b), and COES (c).

3.7. Analysis of Column Bleeding before and after Salt Injection

To determine whether the samples containing LiPF_6 salt cause excessive column bleeding, an experiment was conducted by injecting a blank acetone sample (considered as the baseline sample) before and after five injections of COES and SBS #2. Figure 7 shows the GC \times GC-FID/chromatograms of acetone before and after injection of salt-containing samples. No changes were observed in the amount of column bleeding, noise, or retention times before and after samples that contained LiPF_6 were analyzed, which suggests that the effects of the LiPF_6 on the GC columns were negligible. The solvent-bleeding also remained unchanged.

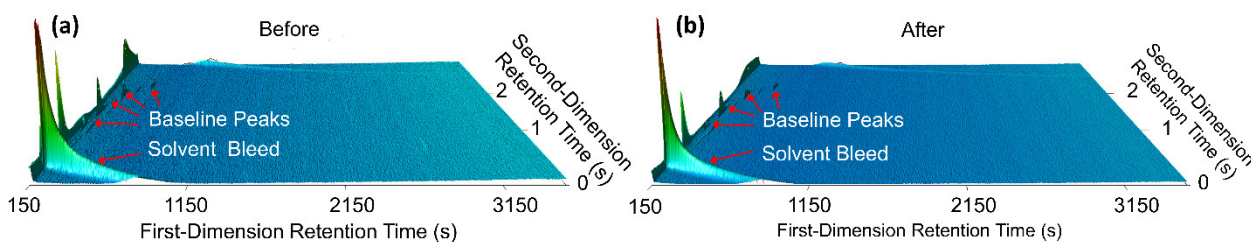


Figure 7. GC \times GC/FID chromatograms of acetone before (a) and after (b) ten samples containing LiPF_6 were analyzed.

As shown in Figure 8, no additional column bleeding or changes in retention times or peak shapes were observed for COES or SBS #2, which further suggests that the effects of the LiPF_6 salt were negligible. This is likely because very little salt was introduced into the instrument (samples were diluted 1000-fold prior to analysis, and only 0.1 μL of the diluted samples was analyzed). Additionally, inlet liners with glass wool were used at the inlet of the GC \times GC instruments to trap nonvolatile compounds, such as LiPF_6 , and the liners were replaced when needed.

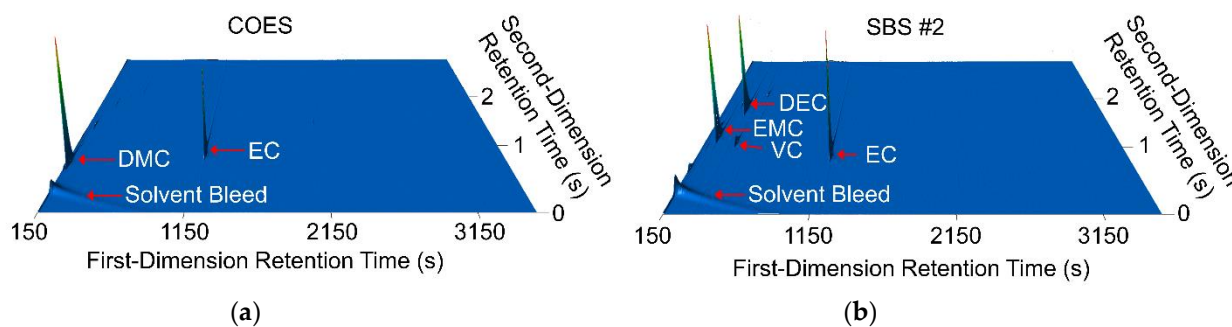


Figure 8. GC \times GC/FID chromatograms of salt-containing samples: (a) COES and (b) SBS #2.

4. Conclusions

Two methods are described to determine the composition of carbonate solvent systems commonly used in Li-ion battery electrolyte solutions, one based on GC \times GC/FID and another based on GC \times GC/EI TOF MS. The accuracy and precision of the methods were tested using various model compound mixtures (MCMs), a commercially obtained electrolyte solution (COES), and single-blind samples (SBSs). Both methods were found to be accurate, precise, and sensitive. The high sensitivity of the methods allowed the use of high dilution factors and low injection volumes, eliminating the need for salt removal. No adverse effects on column bleeding, retention times, or GC peak shapes were observed while analyzing samples containing LiPF_6 salt. The methods employed in this study will be used in future studies to investigate changes in the composition of electrolyte solutions from Li-ion batteries over time, after calendar aging, and after cycle aging.

Author Contributions: Conceptualization, G.K. and J.K.O.; methodology, M.P., L.E.C.-M., B.A.M., H.I.K., G.K. and J.K.O.; formal analysis, M.P., L.E.C.-M. and B.A.M.; investigation, M.P., L.E.C.-M. and B.A.M.; resources, H.I.K., G.K. and J.K.O.; data curation, M.P., L.E.C.-M. and B.A.M.; writing—original draft preparation, M.P., L.E.C.-M. and B.A.M.; writing—review and editing, M.P., L.E.C.-M., B.A.M., H.I.K., G.K. and J.K.O.; visualization, M.P.; supervision, H.I.K., G.K. and J.K.O.; project administration, H.I.K., G.K. and J.K.O.; funding acquisition, G.K. and J.K.O. All authors have read and agreed to the published version of the manuscript.

Funding: This research received no external funding.

Institutional Review Board Statement: Not applicable.

Informed Consent Statement: Not applicable.

Data Availability Statement: The authors confirm that the data supporting the findings of this study are available within the article.

Acknowledgments: The authors would like to gratefully acknowledge the Purdue Polytechnic Institute for providing funding for M. Parhizi to conduct this research. The authors also acknowledge Kyle R. Crompton for preparing single-blind samples (SBS#1 and SBS#2) used for analysis in the present study.

Conflicts of Interest: The authors declare no conflict of interest.

References

1. Goodenough, J.B.; Park, K.S. The Li-ion rechargeable battery: A perspective. *J. Am. Chem. Soc.* **2013**, *135*, 1167–1176. [[CrossRef](#)] [[PubMed](#)]
2. Shah, K.; Balsara, N.; Banerjee, S.; Chintapalli, M.; Cocco, A.; Chiu, W.K.S.; Lahiri, I.; Martha, S.K.; Mistry, A.; Mukherjee, P.P.; et al. State of the Art and Future Research Needs for Multiscale Analysis of Li-Ion Cells. *J. Electrochem. Energy Convers. Storage* **2017**, *14*, 020801. [[CrossRef](#)]
3. Scrosati, B.; Garche, J. Lithium batteries: Status, prospects and future. *J. Power Sources* **2010**, *195*, 2419–2430. [[CrossRef](#)]
4. Parhizi, M.; Ahmed, M.; Jain, A. Determination of the core temperature of a Li-ion cell during thermal runaway. *J. Power Sources* **2017**, *370*, 27–35. [[CrossRef](#)]
5. Wang, Q.; Mao, B.; Stolarov, S.I.; Sun, J. A review of lithium ion battery failure mechanisms and fire prevention strategies. *Prog. Energy Combust. Sci.* **2019**, *73*, 95–131. [[CrossRef](#)]
6. Rothermel, S.; Evertz, M.; Kasnatscheew, J.; Qi, X.; Grütze, M.; Winter, M.; Nowak, S. Graphite Recycling from Spent Lithium-Ion Batteries. *ChemSusChem* **2016**, *9*, 3473–3484. [[CrossRef](#)]
7. Horsthemke, F.; Friesen, A.; Mönnighoff, X.; Stenzel, Y.P.; Grütze, M.; Andersson, J.T.; Winter, M.; Nowak, S. Fast screening method to characterize lithium ion battery electrolytes by means of solid phase microextraction—gas chromatography—mass spectrometry. *RSC Adv.* **2017**, *7*, 46989–46998. [[CrossRef](#)]
8. Ellis, L.D.; Buteau, S.; Hames, S.G.; Thompson, L.M.; Hall, D.S.; Dahn, J.R. A New Method for Determining the Concentration of Electrolyte Components in Lithium-Ion Cells, Using Fourier Transform Infrared Spectroscopy and Machine Learning. *J. Electrochem. Soc.* **2018**, *165*, A256–A262. [[CrossRef](#)]
9. Gachot, G.; Ribière, P.; Mathiron, D.; Grugeon, S.; Armand, M.; Leriche, J.-B.; Pilard, S.; Laruelle, S. Gas Chromatography/Mass Spectrometry as a Suitable Tool for the Li-Ion Battery Electrolyte Degradation Mechanisms Study. *Anal. Chem.* **2011**, *83*, 478–485. [[CrossRef](#)]
10. Gachot, G.; Grugeon, S.; Jimenez-Gordon, I.; Eshetu, G.G.; Boyanov, S.; Lecocq, A.; Marlair, G.; Pilard, S.; Laruelle, S. Gas chromatography/Fourier transform infrared/mass spectrometry coupling: A tool for Li-ion battery safety field investigation. *Anal. Methods* **2014**, *6*, 6120–6124. [[CrossRef](#)]
11. Schultz, C.; Vedder, S.; Streipert, B.; Winter, M.; Nowak, S. Quantitative investigation of the decomposition of organic lithium ion battery electrolytes with LC-MS/MS. *RSC Adv.* **2017**, *7*, 27853–27862. [[CrossRef](#)]
12. Petibon, R.; Rotermund, L.; Nelson, K.J.; Gozdz, A.S.; Xia, J.; Dahn, J.R. Study of Electrolyte Components in Li Ion Cells Using Liquid-Liquid Extraction and Gas Chromatography Coupled with Mass Spectrometry. *J. Electrochem. Soc.* **2014**, *161*, A1167–A1172. [[CrossRef](#)]
13. Terborg, L.; Weber, S.; Passerini, S.; Winter, M.; Karst, U.; Nowak, S. Development of gas chromatographic methods for the analyses of organic carbonate-based electrolytes. *J. Power Sources* **2014**, *245*, 836–840. [[CrossRef](#)]
14. Thompson, L.M.; Stone, W.; Eldesoky, A.; Smith, N.K.; McFarlane, C.R.M.; Kim, J.S.; Johnson, M.B.; Petibon, R.; Dahn, J.R. Quantifying Changes to the Electrolyte and Negative Electrode in Aged NMC532/Graphite Lithium-Ion Cells. *J. Electrochem. Soc.* **2018**, *165*, A2732–A2740. [[CrossRef](#)]
15. Weber, W.; Kraft, V.; Grütze, M.; Wagner, R.; Winter, M.; Nowak, S. Identification of alkylated phosphates by gas chromatography-mass spectrometric investigations with different ionization principles of a thermally aged commercial lithium ion battery electrolyte. *J. Chromatogr. A* **2015**, *1394*, 128–136. [[CrossRef](#)] [[PubMed](#)]

16. Abraham, D.; Roth, E.; Kostecki, R.; McCarthy, K.; MacLaren, S.; Doughty, D. Diagnostic examination of thermally abused high-power lithium-ion cells. *J. Power Sources* **2006**, *161*, 648–657. [[CrossRef](#)]
17. Lamb, J.; Orendorff, C.J.; Roth, E.P.; Langendorf, J. Studies on the Thermal Breakdown of Common Li-Ion Battery Electrolyte Components. *J. Electrochem. Soc.* **2015**, *162*, A2131–A2135. [[CrossRef](#)]
18. Lammer, M.; Königseder, A.; Hacker, V. Holistic methodology for characterisation of the thermally induced failure of commercially available 18650 lithium ion cells. *RSC Adv.* **2017**, *7*, 24425–24429. [[CrossRef](#)]
19. Golubkov, A.W.; Fuchs, D.; Wagner, J.; Wiltsche, H.; Stangl, C.; Fauler, G.; Voitic, G.; Thaler, A.; Hacker, V. Thermal-runaway experiments on consumer Li-ion batteries with metal-oxide and olivin-type cathodes. *RSC Adv.* **2014**, *4*, 3633–3642. [[CrossRef](#)]
20. Zanella, D.; Focant, J.F.; Franchina, F.A. 30th Anniversary of comprehensive two-dimensional gas chromatography: Latest advances. *Anal. Sci. Adv.* **2021**, *2*, 213–224. [[CrossRef](#)]
21. Currie, L.A. Nomenclature in evaluation of analytical methods including detection and quantification capabilities:(IUPAC Recommendations 1995). *Anal. Chim. Acta* **1999**, *391*, 105–126. [[CrossRef](#)]
22. Moffat, R.J. Describing the uncertainties in experimental results. *Exp. Therm. Fluid Sci.* **1988**, *1*, 3–17. [[CrossRef](#)]
23. Devore, J.L. *Probability and Statistics for Engineering and the Sciences*; Cengage Learning: Boston, MA, USA, 2015.